Journal of the European Ceramic Society xxx (xxxx) xxx–xxx

Contents lists available at ScienceDirect

Journal of the European Ceramic Society

journal homepage: www.elsevier.com/locate/jeurceramsoc

Short communication

Annealing effects on the pore structures and mechanical properties of porous alumina via directional freeze-casting

Yufei Tang*, Mengchen Mao, Sha Qiu, Cong Wu

Department of Materials Science and Engineering, Xi'an University of Technology, Xi'an 710048, PR China

ARTICLE INFO

Keywords:
Directional freeze casting
Annealing
Porous alumina
Pore structure
Compressive strength

ABSTRACT

The effects of the annealing methods and annealing temperatures on the pore structures and mechanical properties of porous alumina were investigated. The amorphisation behavior and solidification behavior of the sucrose solutions during annealing were discussed. The pore morphology of porous alumina changed noticeably after uniform annealing. As annealing temperature increased from −25 ℃ to −5 ℃, the pore morphology of porous alumina changed gradually from irregular lamellar channels to circular channels. After directional annealing, the pore morphology of porous alumina was similar to that after uniform annealing; however, the uniformity of pore channels and the density of pore walls were increased. During directional annealing at −15℃, the compressive strength of porous alumina reached 58.8 MPa, which was 35% higher than that of unannealed porous alumina.

1. Introduction

Porous ceramics prepared via freeze-casting can achieve higher compressive strength than porous ceramics prepared using other methods because of their directional pore channels [1,2]. The former has a wide range of applications in bone implant materials, high-temperature filtration, and fuel cells [3,4]. The mechanical properties of this type of porous ceramics mainly depend on their porosity, pore size, and pore distribution [5,6]. Porosity is primarily determined based on the solid content of the slurry [7], whereas pore size and pore distribution are closely related to the preparation process [8,9]. At present, many studies have focused on controlling the pore size and pore distribution of porous ceramics [10–12], such as by inducing the electric field and magnetic field in the freeze-casting process [13,14] and by adding inorganic salts and glycerol to the slurry [15,16]. Changing the freezing temperature is the most effective means to adjust the pore size of porous ceramics [17]. The supercooling degree of the slurry and the nucleation ratio increase as freezing temperature decreases, and thus, small directional crystals can be obtained [18]. However, certain solvents are crystallized in situ instead of demonstrating directional growth when the freezing temperature is too low [19], which decreases the porosity of porous ceramics.

In the pharmaceutical field, ice crystals that formed during the freezing process of the liquid exhibit different shapes and uneven size and distribution, thereby resulting in considerable flow resistance during the drying process and low drying efficiency [20]. To solve the above-mentioned problems, a sucrose solution was used and the annealing process was performed before drying. In this manner, the drying rate can be improved because annealing can change the morphology and distribution of ice crystals, and consequently, the morphology of the amorphous matrix [21,22]. Annealing is also used to eliminate residual stress, reduce deformation and crack tendency, and refine grains during metal heat treatment [23]. Therefore, if the annealing process is introduced into the freeze-casting process to fabricate porous ceramics, then the morphology of solvent crystals can be changed, thereby changing the pore structure and mechanical properties of porous ceramics.

In the current study, sucrose solutions were used as the freezing medium for the alumina slurry. The frozen slurry was annealed after directional freezing, which led to the softening and redistribution of the sucrose solutions. Consequently, the pore structure of the porous alumina was changed. The effects of the annealing methods and annealing temperatures on the pore structures and mechanical properties of porous alumina were investigated. The amorphisation behavior and solidification behavior of the sucrose solutions during annealing was discussed. The compressive strength of porous alumina was also tested. The result of this study provides an important reference for improving the mechanical properties of porous ceramics.

* Corresponding author at: 5 South Jinhua Road, Xi'an, Shaanxi, 710048, PR China.
E-mail address: yftang@xaut.edu.cn (Y. Tang).

https://doi.org/10.1016/j.jeurceramsoc.2018.04.038
Received 5 February 2018; Received in revised form 17 April 2018; Accepted 17 April 2018

2. Experimental procedures

2.1. Materials and methods

Alumina powder (GW-1, Zhengzhou Dengfeng Materials Co. Ltd., Zhengzhou, China) was used as the starting material, and distilled water was used as the freezing medium. Sucrose (AR, Alfa Aesar, Massachusetts, U.S.) was used as the additive for annealing. Carboxymethyl cellulose (CMC, Tianjin Fuchen Chemical Reagents Factory, Tianjin, China) and sodium polyacrylate (PAAS, Sinopharm Chemical Reagent Co., Ltd., Shanghai, China) were used as the binder and dispersant, respectively.

Alumina powder was mixed with 2 wt.% PAAS, 1 wt.% CMC, and 20 wt.% sucrose in distilled water. Then, the resulting mixture was ground with a ball mill for 24 h to obtain alumina slurry (with a solid content of 20 vol.%). The slurry was injected into cylindrical molds and frozen directionally using a −75 °C cold source for 3 h. After the slurry was completely frozen, it was annealed at −5 °C, −15 °C, and −25 °C, and then refrozen at −75 °C. The refrozen slurry was dried in a freeze-dryer (TRID 2.5 L, LABCONCO FreeZone®, Kansas, U.S.) for 24 h. Finally, porous alumina was obtained after being sintered at 1600 °C for 2 h. The heating and cooling rates were 5 °C/min.

Sucrose is a non-reductive disaccharide that exhibits amorphous transition but not crystallization during cooling. It is an effective, and in fact, the most commonly used protective agent for freeze-drying [24]. The amorphous transition temperature (T_g') of sucrose solution is −32.5 °C [20], and the annealing temperature is generally higher than T_g'. Accordingly, −5 °C, −15 °C, and −25 °C were selectedas the annealing temperatures in this study. Annealing methods were divided into uniform annealing and directional annealing (Fig. 1). In uniform annealing, the frozen slurry was sealed and then placed in a liquid cold source (i.e., low-temperature ethanol) for annealing and refreezing. In directional annealing, annealing and refreezing were directed from the cold source toward the top.

2.2. Characterization

The morphology of porous alumina was characterized using a scanning electron microscope (JSM 6390 A, JEOL, Japan). The lamellar spaces of porous alumina were determined by measuring the cross-section of the samples in the SEM images with SmileView (Software, JEOL, Japan). A total of 100 pore channels were tested in this manner to obtain the lamellar spacing distribution. Viscosities of the saturated sucrose solution with different freezing temperature were measured with a viscometer (SNB-2, Shanghai Nirun Intelligent Technology Co., Ltd., Shanghai, China). A differential thermal analyzer (DSC-204, NETZSCH, Germany) was used to measure the thermal changes of the ceramic slurry with the sucrose solution during the freezing and annealing processes. The heating and cooling rates were 1 °C/min under the protection of argon. The open porosity of porous alumina was measured based on the standard ASTM C20 (Standard Test Methods for apparent porosity, water absorption, apparent specific gravity, and bulk density of burned refractory brick). The compressive strength of porous alumina was measured on cylindrical samples with Φ7 × 11 mm using a computer servo to control the material testing machine (HT-2402-100KN, Hungta, Taiwan). Ten samples were tested to obtain an average value.

3. Results and discussion

When the frozen slurry was heated to over T_g' for annealing, the molecules in the vitreous body could be moved and rotated. Amorphous transition occurred from a non-equilibrium glass state to a softened state [25]. The mobility of molecules increased with an increase in temperature. After refreezing, the softening part was refrozen, but the structure was rearranged. A liquid cold source was used for uniform annealing. The morphologies of porous alumina obtained at different annealing temperatures are shown in Fig. 2. When the annealing temperature was −25 °C, lamellar pore channels were maintained, but several large channels were observed. The lamellar spaces between pore walls were uneven, and a large number of small pores were distributed between lamellar channels from the longitudinal section (Fig. 2d–f). Viscosities of the saturated sucrose solution with different freezing temperature were measured (Fig. 3). The sucrose solution showed a rubbery state and no fluidity when the temperature below −20 °C, and the viscosity value could not be performed. After continuously heated to −15 °C, the rubbery state was changed to viscous state. The deformation of the sucrose molecular was gradually increased with fluidity. The viscosity of the sucrose solution was 1681 mPa·s. The viscosity was reduced to 194.5 mPa s at −5 °C. The viscosity of sucrose solution was decreased with the increasing temperature in annealing. Therefore, it is inferred that the softening degree and fluidity of alumina frozen body were increased with the high temperature. Sucrose molecules were easy redistribute in melting state and changing the pore morphology in high annealing temperatures. The annealing temperature at −25 °C was close to T_g', the viscosity of the softened amorphous body was high (unable to be measured), and molecular activity was limited. Inadequate annealing caused the softening part to gather only near the original position. After refreezing, several large frozen bodies were formed. When the annealing temperature was −15 °C, small and uniform lamellar pores (about 20 μm) were observed and several bridges were found in the pore channels. The mobility of sucrose molecules was increased, and annealing was sufficient. The decreased viscosity of the softened sucrose solution was beneficial for redistribution. When the annealing temperature was increased to −5 °C, the pore size of porous alumina was evidently increased to about 40 μm, and some of the pores were circular. The viscosity of the softened sucrose solution was low (194.5 mPa·s), molecular mobility was active, and the driving force of diffusion was increased. After refreezing, circular pores were formed due to the minimum surface

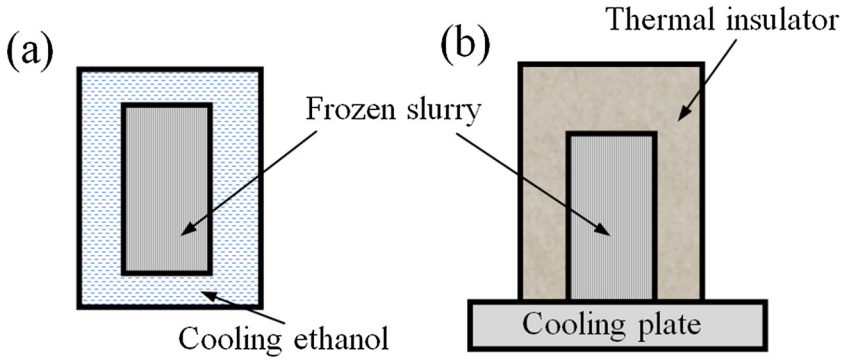

Fig. 1. Schematic of annealing methods for slurries with sucrose solutions after freezing: (a) uniform annealing and (b) directional annealing.

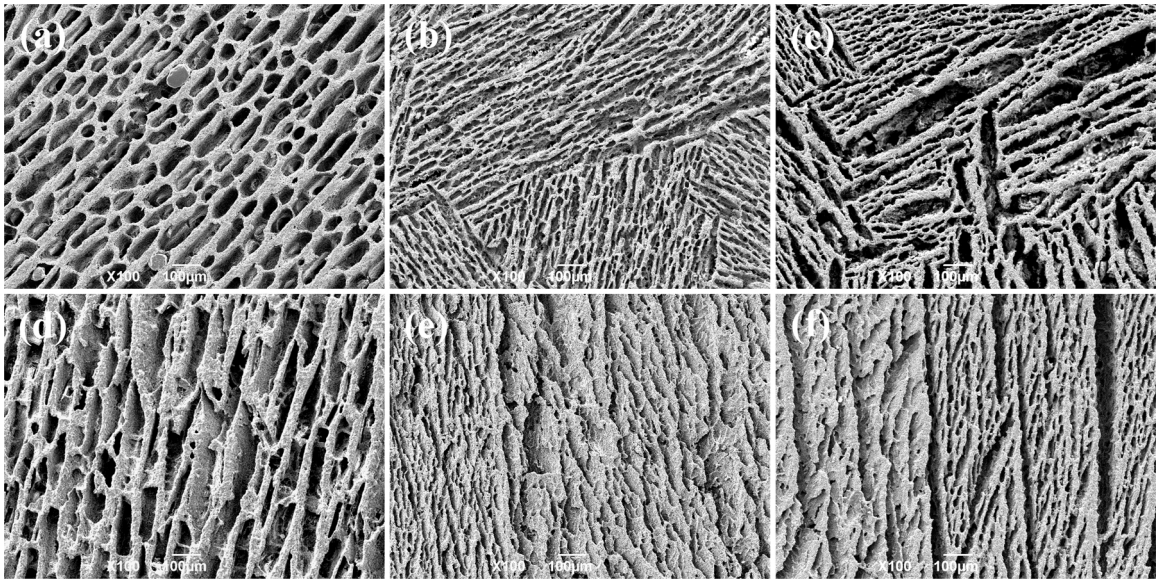

Fig. 2. Morphologies of porous alumina after the uniform annealing of frozen sucrose solutions at different annealing temperatures: (a)–(d) −5 °C, (b)–(e) −15 °C, and (c)–(f) −25 °C; (a)–(c) cross-section morphologies and (d)–(f) longitudinal section morphologies.

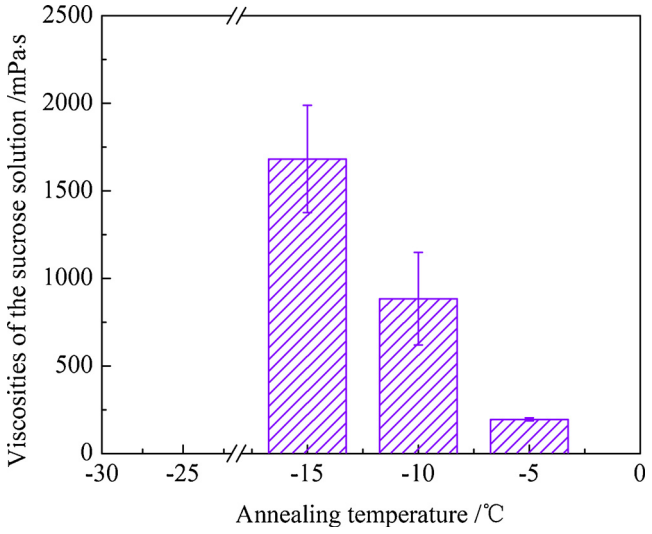

Fig. 3. Viscosities of the saturated sucrose solution with different freezing temperature.

energy.

The pore morphology of porous alumina was considerably changed after uniform annealing. From the view of the longitudinal section, however, numerous pore channels that were inconsistent with the freezing direction were found, particularly when the annealing temperature was −25 °C and −15 °C (Fig. 2f and e), which could be attributed to the random freezing direction during refreezing. This phenomenon may reduce the mechanical properties of porous alumina, and thus, we consider designing a new annealing method, namely, directional annealing.

The pore morphology of porous alumina that was obtained after directional annealing is shown in Fig. 4. The cross-section morphology of porous alumina obtained via directional annealing is similar to that obtained via uniform annealing (Fig. 4a–c), but the uniformity of pore sizes is found. Lamellar spacing distribution of porous alumina for different annealing processes and different temperatures were characterized (Fig. 5). The lamellar spacing distribution was range from 10 to 40 μm when using the directional annealing process at different temperatures (Fig. 5b). On the contrary, porous alumina obtained after uniform annealing process had wide ranges of lamellar spacing distribution with different annealing temperature (Fig. 5a).

Viscosities of the amorphous body were gradually changed (Fig. 3). When the annealing temperature was −15 °C, porous alumina exhibited a lamellar pore structure and clear pore walls (Fig. 4e). When the annealing temperature was increased to −5 °C, the softened sucrose solution demonstrated exceptional fluidity, and a large number of circular pore channels were formed (Fig. 4a), the circular pore sizes were about 28 μm. After directional annealing, directional lamellar pore channels were produced, which could be beneficial for improving the mechanical properties of porous alumina ceramics.

The thermal analysis of the slurry with 20 wt.% sucrose solution was conducted to investigate its thermal change during directional freezing and annealing. The results are presented in Fig. 6. The alumina slurry achieved an evident exothermic peak near −22 °C during directional freezing (Fig. 6a). This result indicated that the sucrose solution in the slurry solidified during the rapid freezing process. When annealing after freezing was completed, the “curvestep” occurring at −38 °C indicated that amorphous transition was realized [26]. When the annealing temperature was over −38 °C, the sucrose solution exhibited amorphous softening. Subsequently, porous alumina with different pore structures could be obtained after the redistribution of the sucrose solution.

The sucrose solution was used as the freezing medium of the alumina slurry. Water was nucleated as ice crystals near the cold source and then directionally grown. Directional growth will push the alumina particles in the slurry toward both sides to form pore walls. The sucrose concentration at the front of the ice crystal growth was gradually increased, and it precipitated around the ice crystals after it was saturated. The high-concentration sucrose solution exhibited amorphous transition, and the resulting sucrose solutions with amorphous state were distributed around the ice crystals (Fig. 6c). When the sucrose solution was in an amorphous state, its viscosity was 10^{14} Pa·s, the molecules were nearly free from fluidity, and the amorphous state was stable. When the annealing temperature is higher than T_g', the viscosity can be estimated according to the Willams–Landel–Ferry equation [27], which is expressed as follows:

$$\log(\eta/\eta_g) = \frac{-C_1(T - T_g)}{C_2 + (T - T_g)}, \quad (1)$$

where η denotes the viscosity at temperature T, η_g indicates the viscosity

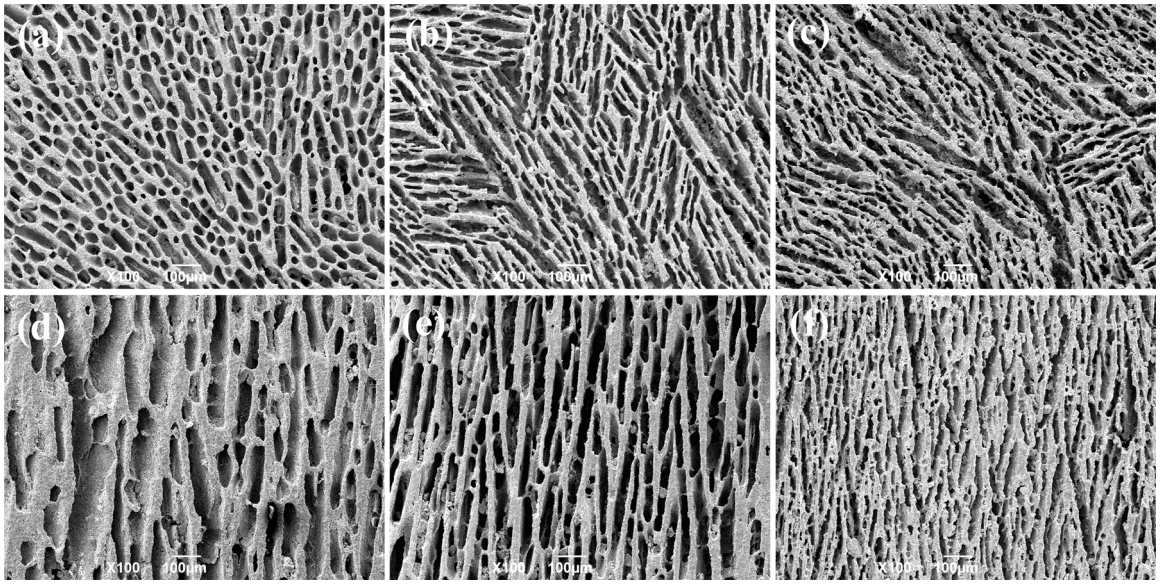

Fig. 4. Morphologies of porous alumina after the directional annealing of frozen sucrose solutions at different annealing temperatures: (a)–(d) −5 °C, (b)–(e) −15 °C, and (c)–(f) −25 °C; (a)–(c) cross-section morphologies and (d)–(f) longitudinal section morphologies.

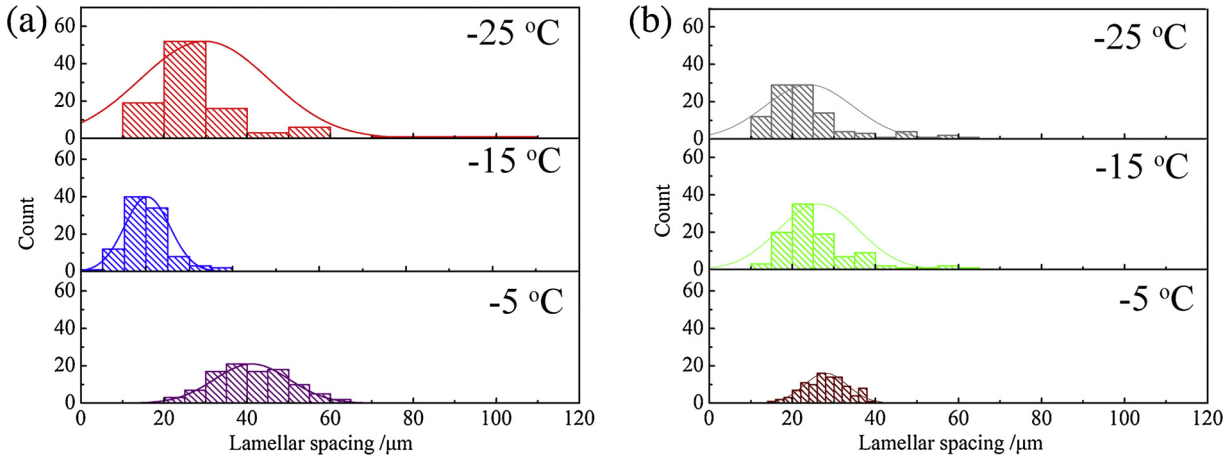

Fig. 5. Lamellar spacing distributions of porous alumina with different annealing processes and different temperature: (a) uniform annealing and (b) directional annealing.

at temperature T_g, and C_1 and C_2 are constants. When a certain amount of sucrose was vitrified, T_g' can be used instead of T_g in the equation. The vitreous body around the ice crystals began to soften when amorphous transition occurred. The sucrose solution transition was similar to a polymer transition to a high-elastic state. The whole sucrose solution exhibited fluidity and was softened by annealing above T_g [28]. The surface of the lamellar ice crystals obtained via directional freezing was rough, and the amorphous body diffused completely and was re-frozen (Fig. 6d).

Fig. 7a shows the open porosity of porous alumina after performing different annealing processes. The open porosity of porous alumina was approximately 60%, which was primarily attributed to the alumina content of the slurry. Fig. 7b shows the compressive strength of porous alumina obtained via different annealing temperatures and annealing methods. The compressive strength of unannealed porous alumina was 43.6 MPa. The compressive strength of porous alumina obtained via uniform annealing at different temperatures was approximately 30 MPa lower than that of the unannealed samples. The main reason for this result was the random freezing directions during the refreezing process. Moreover, several pore channels were inconsistent with directional freezing. High compressive strength can be achieved via directional annealing. The compressive strength of porous alumina obtained via directional annealing at −15 °C could reach up to 58.8 MPa because the pore walls were dense and lamellar spacing was uniform (Fig. 4e); hence, stress concentration was not formed. However, the compressive strength of porous alumina obtained via directional annealing at −25 °C was low because annealing was inadequate and the distribution of pore channels was not uniform (Fig. 4f). Directional annealing at −15 °C cannot only improved the uniformity of porous ceramics, but also theircompressive strength.

4. Conclusions

Alumina slurry was prepared using sucrose solutions as the freezing medium, and porous alumina was fabricated via directional freeze-casting. After the slurry was frozen, uniform annealing and directional annealing were performed. The annealing process significantly affected the pore structure of porous alumina. As the annealing temperature increased from −25 °C to −5 °C, pore morphology changed but the density of pore walls was low because the direction was random during the refreezing process after annealing. The uniformity of lamellar spaces and the density of pore walls were increased via directional

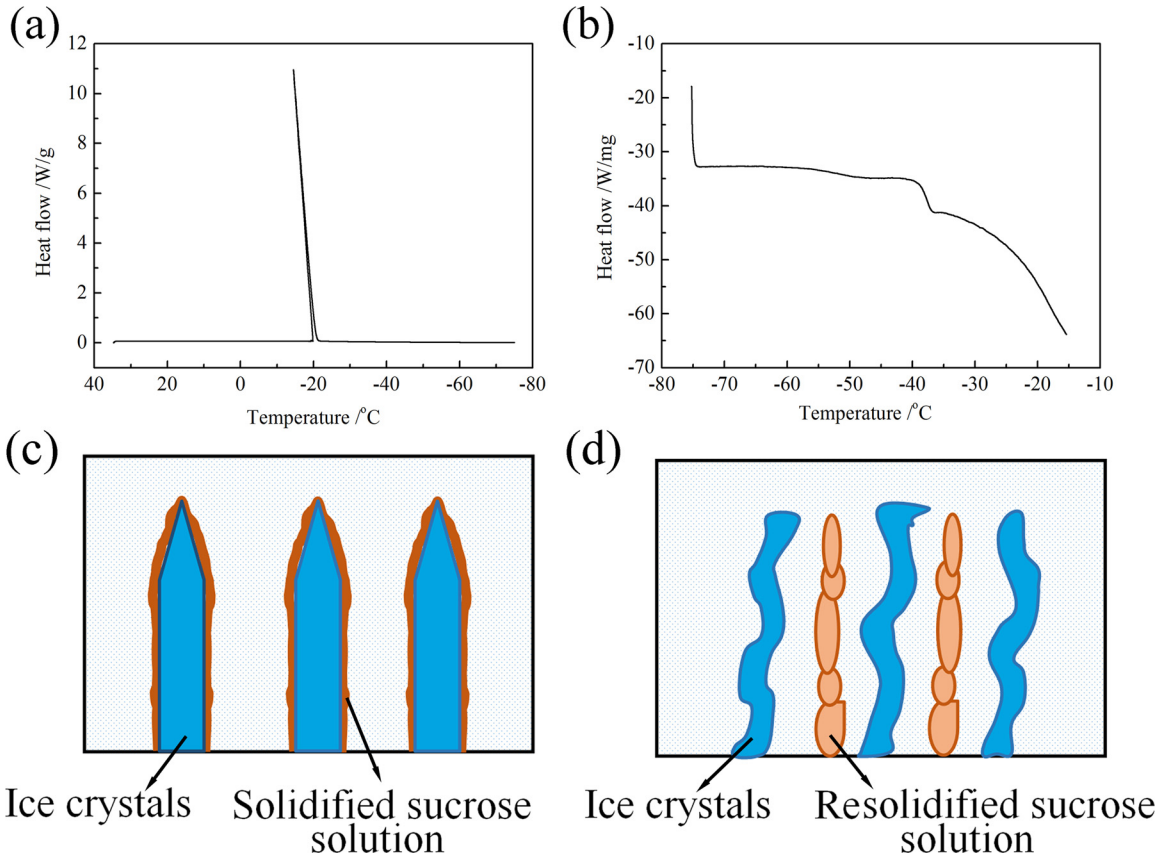

Fig. 6. Differential scanning calorimetry curves and solidification behavior mechanism of alumina slurries with sucrose solutions: (a)–(c) freezing process and (b)–(d) annealing after freezing.

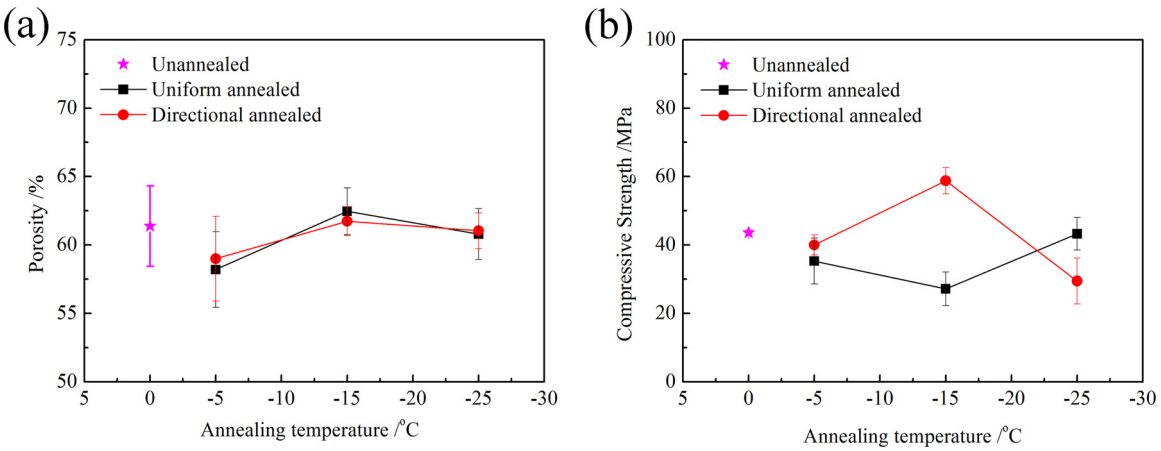

Fig. 7. Open porosities and compressive strengths of porous alumina after different annealing processes: (a) open porosities and (b) compressive strengths.

annealing and refreezing. When directional annealing was performed at −15 °C, the compressive strength of porous alumina was 58.8 MPa, which was 35% higher than that of unannealed porous alumina. The directional annealing process can improve the pore uniformity and compressive strength of porous ceramics. However, the influence of different sucrose content in slurries on the pore structure and mechanical properties of porous ceramics needs further study. Besides, applications of sucrose in ceramic slurries with different solvent systems may also be explored.

Acknowledgments

The authors would like to acknowledge the support from the National Natural Science Foundation of China (No. 51572217), the China Postdoctoral Science Foundation (No. 2016T90937) and the Natural Science Foundation of Shaanxi Province (2016JQ5058).

References

[1] S. Deville, E. Saiz, R.K. Nalla, A.P. Tomsia, Freezing as a path to build complex composites, Science 311 (2006) 515–518.
[2] A.A. Al-Attar, M.A. Zaeem, S.A. Ajeel, N.E.A. Latiff, Effects of SiC, SiO_2, and CNTs nanoadditives on the properties of porous alumina-zirconia ceramics produced by a hybrid freeze casting-space holder method, J. Eur. Ceram. Soc. 37 (2016) 1635–1642.
[3] T.L. Cable, S.W. Sofie, A symmetrical, planar SOFC design for NASA's high specific power density requirements, J. Power Sources 174 (2007) 221–227.
[4] S. Deville, E. Saiz, A.P. Tomsia, Freeze casting of hydroxyapatite scaffolds for bone

tissue engineering, Biomaterials 27 (2006) 5480–5489.
[5] Y. Tang, Q. Miao, S. Qiu, K. Zhao, L. Hu, Novel freeze-casting fabrication of aligned lamellar porous alumina with a centrosymmetric structure, J. Eur. Ceram. Soc. 34 (2014) 4077–4082.
[6] G. Liu, D. Zhang, C. Meggs, T.W. Button, Porous Al_2O_3–ZrO_2, composites fabricated by an ice template method, Scripta. Mater. 62 (2010) 466–468.
[7] F. Ye, J. Zhang, L. Liu, H. Zhan, Effect of solissssd content on pore structure and mechanical properties of porous silicon nimide ceramics produced by freeze casting, Mater. Sci. Eng. A 528 (2011) 1421–1424.
[8] B.H. Yoon, E.J. Lee, H.E. Kim, Y.H. Koh, Highly aligned porous silicon carbide ceramics by freezing polycarbosilane/camphene solution, J. Am. Ceram. Soc. 90 (2007) 1753–1759.
[9] L. Hu, C.A. Wang, Y. Huang, C. Sun, S. Lu, Control of pore channel size during freeze casting of porous YSZ ceramics with unidirectionally aligned channels using different freezing temperatures, J. Eur. Ceram. Soc. 30 (2010) 3389–3396.
[10] S. Deville, E. Maire, A. Lasalle, A. Bogner, C. Gauthier, J. Leloup, C. Guizard, Influence of particle size on ice nucleation and growth during the ice-templating process, J. Am. Ceram. Soc. 93 (2010) 2507–2510.
[11] Y. Tang, S. Qiu, C. Wu, Q. Miao, K. Zhao, Freeze cast fabrication of porous ceramics using tert-butyl alcohol–water crystals as template, J. Eur. Ceram. Soc. 36 (2016) 1513–1518.
[12] T. Moritz, H.J. Richter, Ceramic bodies with complex geometries and ceramic shells by freeze casting using ice as mold material, J. Am. Ceram. Soc. 89 (2006) 2394–2398.
[13] Y. Zhang, L. Hu, J. Han, Preparation of a dense/porous bilayered ceramic by applying an electric field during freeze casting, J. Am. Ceram. Soc. 92 (2009) 1874–1876.
[14] Y. Tang, S. Qiu, Q. Miao, C. Wu, Fabrication of lamellar porous alumina with axisymmetric structure by directional solidification with applied electric and magnetic fields, J. Eur. Ceram. Soc. 36 (2016) 1233–1240.
[15] E. Munch, E. Saiz, A.P. Tomsia, S. Deville, Architectural control of freeze-cast ceramics through additives and templating, J. Am. Ceram. Soc. 92 (2009) 1534–1539.
[16] Y. Zhang, L. Hu, J. Han, Z. Jiang, Freeze casting of aqueous alumina slurries with glycerol for porous ceramics, Ceram. Int. 36 (2010) 617–621.
[17] S.W. Yook, H.D. Jung, C.H. Park, K.H. Shin, Y.H. Koh, Y. Estrin, H.E. Kim, Reverse freeze casting: a new method for fabricating highly porous titanium scaffolds with aligned large pores, Acta Biomater. 8 (2012) 2401–2410.
[18] K. Zhao, Y. Tang, Y. Qin, J. Wei, Porous hydroxyapatite ceramics by ice templating: freezing characteristics and mechanical properties, Ceram. Int. 37 (2011) 635–639.
[19] N.A.S. Zairani, M. Jaafar, N. Ahmad, K.A. Razak, Fabrication and characterization of porous β-tricalcium phosphate scaffolds coated with alginate, Ceram. Int. 42 (2016) 5141–5147.
[20] J. Searles, J. Carpenter, T. Randolph, Annealing to optimize the primary drying rate, reduce freezing-induced drying rate heterogeneity, and determine Tg' in pharmaceutical lyophilization, J. Pharm. Sci-US. 90 (2001) 872–887.
[21] M.E. Sahagian, H.D. Goff, Effect of freezing rate on the thermal, mechanical and physical aging properties of the glassy state in frozen sucrose solutions, Thermochim. Acta 246 (1994) 271–283.
[22] W. Wang, Lyophilization and development of solid protein pharmaceuticals, Int. J. Pharm. 203 (2006) 1–60.
[23] Y. Zhang, A. Gokhman, W. Wang, Z. Zhang, Effects of annealing on grain-boundary character distribution and texture evolution in hot-rolled Fe-6.5 wt% Si steel, J. Magn. Magn. Mater. 451 (2018) 187–192.
[24] L. Kreilgaard, S. Frokjaer, J.M. Flink, T.W. Randolph, J.F. Carpenter, Effects of additives on the stability of humicola lanuginosa lipase during freeze-drying and storage in the dried solid, J. Pharm. Sci-US. 88 (1999) 281–290.
[25] J.Y. Lim, D.G. Lim, K.H. Kim, S.K. Park, S.H. Jeong, Effects of annealing on the physical properties of therapeutic proteins during freeze drying process, Int. J. Biol. Macromol. 107 (2018) 730–740.
[26] J.A. Searles, J.F. Carpenter, T.W. Randolph, The ice nucleation temperature determines the primary drying rate of lyophilization for samples frozen on a temperature controlled shelf, J. Pharm. Sci-US. 90 (2001) 860–871.
[27] M.L. Williams, R.F. Landel, J.D. Ferry, The temperature dependence of relaxation mechanisms in amorphous polymers and other glass-forming liquids, J. Am. Chem. Soc. 77 (1955) 3701–3707.
[28] S.A. Luthra, I.M. Hodge, M.J. Pikal, Investigation of the impact of annealing on global molecular mobility in glasses: optimization for stabilization of amorphous pharmaceuticals, J. Pharm. Sci-US. 97 (2008) 3865–3882.